

**STRONG ENHANCEMENT OF DD-REACTION ACCOMPANIED
BY X-RAY GENERATION IN A PULSED LOW VOLTAGE
HIGH-CURRENT DEUTERIUM GLOW DISCHARGE
WITH A TI-CATHODE**

A.G. LIPSON AND G.H. MILEY

*Department of Nuclear, Plasma & Radiological Engineering
University of Illinois at Urbana-Champaign, Urbana, IL 61801 USA*

A.S. ROUSSETSKI

*P.N. Lebedev Physics Institute
The Russian Academy of Sciences, Moscow 117924, Russia*

A.B. KARABUT

State Scientific-Industrial Association "Luch", Podol'sk, Moscow Region 142100, Russia

Using noiseless solid-state CR-39 plastic track and $\text{Al}_2\text{O}_3:\text{C}$ thermo-luminescent detectors, the yields of 3.0 MeV protons from DD-reaction and soft x-ray photons emitted from the cathode were studied in the periodic pulsing deuterium glow discharge with titanium cathodes at low discharge voltages (in the range 0.8–2.5 kV) and high current density (300–600 mA/cm²). The analysis of DD-proton yield versus accelerating voltages allowed us to estimate the deuteron screening potential value U_S in the deuteron energy range of $0.8 < E_d < 2.45$ keV. A strong DD-reaction enhancement was found in the glow discharge (the effective screening potential $U_e = 610 \pm 150$ eV was found) compared to that for accelerator experiments at higher deuteron energies ($E_{\text{lab}} \geq 2.5$ keV) and lower beam current density (50–500 $\mu\text{A}/\text{cm}^2$). X-ray measurements showed an intense ($I_x = 10^{13} - 10^{14} \text{ s}^{-1}\text{cm}^{-2}$) soft x-ray emission (with a mean energy $E_x = 1.2 - 1.5$ keV) directly from the titanium cathode. The x-ray yield is strongly dependent on the deuterium diffusivity in the near the surface layer of cathode.

1. Introduction

Accelerator experiments performed recently¹⁻⁹ at relatively low projectile energies ($(E_{\text{pr}})_{\text{lab}} \leq 5.0$ keV) show the presence of non-negligible screening effects in the majority of metallic targets, in particular under bombardment with deuterons. It should be noted that experimental studies of fusion reactions in metal targets using light nuclei indicate an exponential enhancement of the reaction probability (or astrophysical S-factor) with a decrease in the projectile energy. Even for gaseous D_2 target bombarded with low-energy deuterons down to $(E_d)_{\text{lab}} = 3.0$ keV, the deduced screening potential $U_e = 25 \pm 5$ eV was, remarkably, found to be higher than the adiabatic limit of the DD-reaction in deuterium molecule ($U_{\text{ad.}} = 14.0$ eV).¹

For most metals and some metal oxides⁶⁻⁹ the experimental DD-reaction enhancement and deduced screening potential U_e are rather larger than those measured for gaseous targets and predicted from the standard approximation of DD-reaction cross-section at low energies.¹⁰ In Ref. [8], the experimental yield of the D(d,p)T reaction for PdO target bombardment with low-energy deuterons down to $E_{\text{lab}} = 2.5$ keV was found to be 50 times higher than that predicted from the standard DD-reaction cross-section deduced from the Bosch and Hale approximation for the DD-reaction yield at a deuteron energy $E_d = 2.5$ keV,¹⁰ corresponding to a screening potential of $U_e = 600$ eV. In the works of Raiola and co-workers^{6,7} the yields of D(d,p)T reaction and screening potentials deduced from the astrophysical factor were studied systematically for about 30 simple elements of periodic table, including both metallic and some non-metallic elements. It was found that majority of studied metals possess a “large” screening potential of $U_e > 100$ eV, excluding, mainly, metals of group 4 (Ti, Zr, Hf) and group 11 (Cu, Ag, Au). The authors^{6,7} did not find any specific experimental conditions or properties of bombarded targets (including accelerator deuteron current density, crystal and electron structure of metals, Z , as well as deuterium diffusivity in the target) that affected the DD-reaction enhancement and increased screening potential. At the same time, it should be noted that the accelerator used in [6,7] allows only a weak deuteron beam current, ranging from 1 to 54 μA , allowing measurements of the deuteron yield only at relatively high deuteron energies ($E_{\text{lab}} > 5.0$ keV).

Kasagi *et al.*^{8,9} recently measured D(d,p)T yields in several metal and metal oxide targets down to $E_d = 2.5$ keV using a low-energy accelerator that operated with a higher beam current (a D^+ beam current in the range 60–400 μA), and found that the screening potential value U_e at such beam intensity is strongly affected by diffusivity of deuterium in metals. In the case of metals possessing a low deuterium diffusivity and a high activation energy for deuteron diffusion (Ti and Au), the screening potentials were found to be low: 65 ± 15 eV and 70 ± 10 eV, respectively. These screening potentials are only two times above that for D_2 gaseous targets. On the other hand, in Pd and PdO targets with high deuterium diffusivity, the screening potentials were found to be $U_e = 310$ and 600 eV, respectively;⁹ sufficiently high so as to be referred to as “gaseous”-like valence electron screening.

So far, the DD-reaction yields in metal targets were studied using only accelerators with relatively low beam currents ($J_d \leq 400 \mu\text{A}$) and deuteron energies $E_d \geq 2.5$ keV. A further decrease in accelerating voltage leads to problems with the beam current that makes it impossible to detect DD-reaction products within a reasonable experimental time, due to the vanishingly small yield. At the same time, the study of DD-reaction yield and cross-section behavior at lower deuteron energies (below the 1.0 keV range) is of a great interest for astrophysical and thermonuclear studies.

An alternative opportunity exists to study DD-reaction yield in the $E_d \leq 1.0$ keV projectile deuteron energy range using a high-current pulsed glow discharge in deuterium. Earlier, it was shown¹¹ that this type of glow discharge can generate

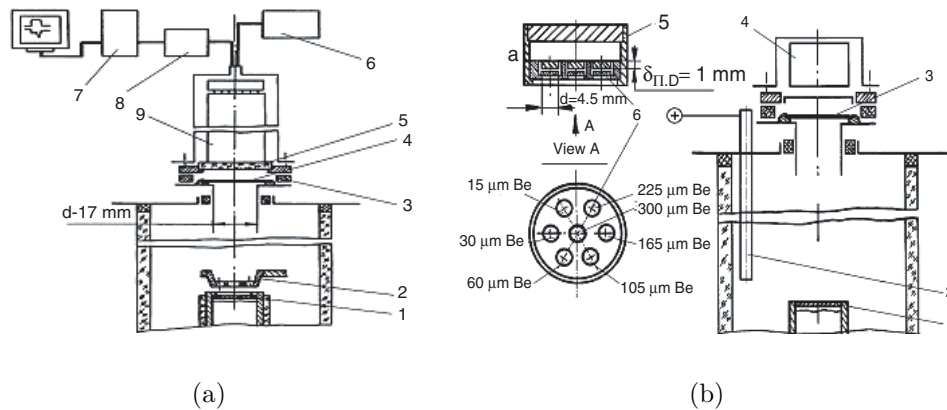


Figure 1. (a) Schematic diagram of glow discharge set up; 1: Ti cathode; 2: Mo anode with holes; 3: insulators; 4–15: μm thick Be-foil; 5: scintillator; 6: PEM power supply; 7: oscilloscope; 8: preamp; 9: PEM. (b) Schematic representation of an “open cathode” experiment. (a) thermoluminescent detectors and absorbing Be screens of various thickness. 1: cathode; 2: anode; 3: Be foil screens; 4: thermoluminescent detectors or obscure camera; 5: metallic cassette to hold the detectors; 6: absorbing Be foil screens with thickness ranging 15–300 μm .

deuterons with energies ranging from 0.8 to 2.5 keV, and current densities ranging from 300–600 mA/cm^2 , at a deuterium pressure in the range of 2 to 10 mm Hg. The current density achieved on a glow discharge deuteron bombardment of the cathode is about three orders of magnitude above that for the best low-energy accelerators. A preliminary estimate shows that high current glow discharge deuteron bombardment of a cathode target could allow detection of the reaction products down to $E_d \leq 1.0$ keV (for about several tens hours of glow discharge operation), assuming that the exponential enhancement of the DD-reaction persists at lower deuteron energy. Moreover, the high-current glow discharge cathode-target bombardment may induce a measurable level of x-ray emission that was predicted for DD-reaction in the lattice environment,¹² and simple x-ray diagnostics may be used to detect it.

In this paper, we show results from a systematic study of DD-reaction and x-ray emission yields during very low-energy deuteron bombardment (in the energy range $0.8 < E_d < 2.45$ keV) of titanium cathodes in a high-current pulsed glow discharge. The results of thick target yield measurements with titanium cathodes allowed us to obtain an unusually high DD-reaction enhancement (about nine orders of magnitude larger compared to the standard Bosch and Hale approximation of DD-reaction cross-section to lower energies) at very low deuteron energies, described by the screening potential $U_e = 610 \pm 150$ eV.

2. Experimental Technique

The in-situ detection of charged particles from DD-reaction and x-rays was carried out in a glow discharge vacuum chamber during discharge operation at different voltages and currents.

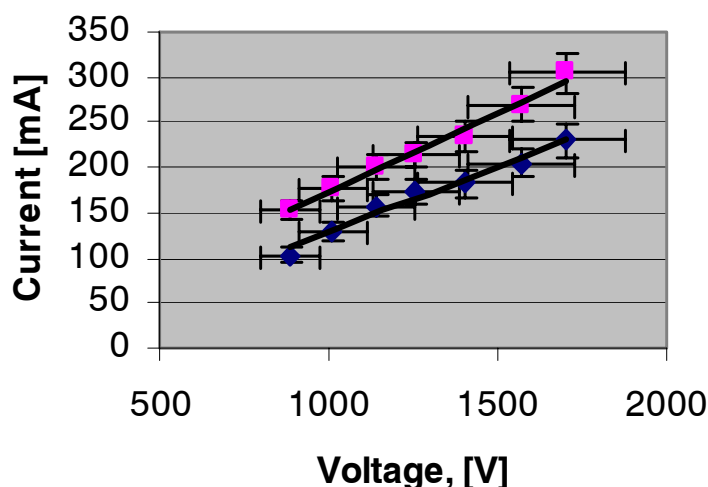


Figure 2. Current and voltage characteristics of glow discharge with a titanium cathode at two deuterium pressures: $p = 4.2$ and 6.0 mm Hg.

2.1. Glow discharge facility

A schematic of the glow discharge facility with appropriate detectors is shown in Figures 1(a) and 1(b). The distance between the massive movable Mo anode, and the removable cathode (thickness $h = 0.01$ cm, area $S = 0.64$ cm²) was varied over 4.0-5.0 mm. During discharge operation, the glow was spread over the entire cathode area, so that the discharge regime used can be considered as an “anomalous” one.^{13,14} The current and voltage repetitive pulses have approximately a square shape, a duration of $\Delta\tau \approx 200$ -400 μ s, a repetition frequency of 5 kHz and a short rise time (less than 1.0 μ s). The pulse parameters were continuously monitored during discharge operation by a 2-channel (divided by U and I channels) 100 MHz memory oscilloscope. The power supply used allowed us to obtain a stable glow discharge regime in the pressure range for deuterium (hydrogen) of $P = 2.0$ –9.0 mm Hg. During the discharge operation, the high current (voltage) fast pulsation has not been typically observed within a 10 ns time resolution. It was found that a strict continuous deuterium pressure stabilization during discharge operation resulted in the stabilization of discharge voltage and current. At the conditions of the quasi-stable glow discharge, the D^+ energy in laboratory system would be exactly equal to the voltage applied, because the very low degree of ionization in this type of glow discharge ($\alpha_i < 10^{-5}$), rules out completely the thermalization of the deuterium plasma.¹³ In this established glow discharge regime, the uncertainty of the mean deuteron energy was found to be $\pm 10\%$ of the nominal voltage, and is determined primarily by small residual instabilities in the discharge voltage and current.

The current and voltage characteristics of the discharge measured at constant

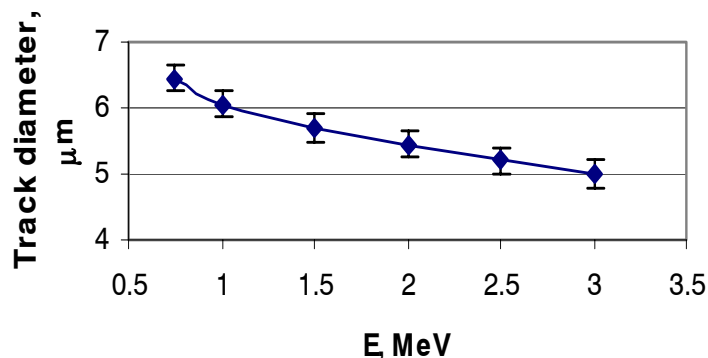


Figure 3. Proton calibration curve (track diameter versus proton energy) obtained by Van de Graaf accelerator bombardment of Fukuvi CR-39 track detectors.

deuterium pressure show a good proportionality between the discharge current and voltages in the ranges 100-300 mA and 800-2000 V, respectively as shown in Figure 2. To obtain the largest DD-reaction yield, maximal currents were chosen at appropriate deuterium pressure to correspond with the voltages employed, in accordance with $V-I$ characteristics presented in Fig. 2.

2.2. Thermistors

A temperature measurement done with thermistors attached to the back-side of the cathode showed a 50-100 K temperature increase during discharge operation.¹⁵ However, this temperature reading was found to be not correct because experiments show traces of melting over the whole cathode surface, under conditions when a minimal input electric power density $P \geq 100 \text{ W/cm}^2$ was used. Thus, we would consider the maximum effective temperature of the titanium cathode subsurface (comparable with the deuteron stopping range) under deuteron bombardment to be melting point of titanium.

2.3. Emulsion detectors

To detect DD-reaction products during the operation of the discharge, several holes were drilled out of the anode body. CR-39 track detectors were placed in the discharge chamber space behind the anode (Fig. 1(a)) at a distance of $R = 3.0$ cm from the cathode surface. Measurements with the similar electrodes, but in hydrogen glow discharge, were used as background experiments.

For charged particle detection (of 3.0 MeV protons from $d(d,p)t$ reactions), purified Fukuvi Chemical plastic CR-39 track detectors were used. These detectors were calibrated (see Figure 3) using standard alpha sources (2.0–7.7 MeV), using a beam of alphas from the cyclotron (in the range of 8.0–30.0 MeV), and using proton

beams in the range of 0.5 to 3.0 MeV from a Van de Graaf accelerator. For the identification of charged particle tracks ($E > 100$ keV/nucleon) the CR-39 detectors were etched in 6N solution of NaOH at $t = 70^\circ\text{C}$ for 7 h. Visualization of tracks and measurement of their diameters were carried out with a microscope equipped with a digital camera. In accordance with the proton calibration, 3.0 MeV protons expected from DD-reaction are located near a track diameter of $5.2 \mu\text{m}$. To prevent the electrode material sputtering, and also to avoid the effect of the deuterium plasma on the CR-39 surface, the detectors were covered by an Al foil $11 \mu\text{m}$ thick, which is transparent for 3.0 MeV protons and high-energy alpha particles. Using the calibration data, we carried out an estimation of the CR-39 detector efficiency with respect to 3.0 MeV protons. Measurements showed that at a cathode to detector distance of $R = 3.0$ cm, the CR-39 efficiency is determined only by the geometrical factor (at normal incidence of protons on the detector¹⁶). Taking into account also the total area of the holes drilled in the anode body, the efficiency of 3.0 MeV proton detection was found to be $\varepsilon_p = 5.6 \times 10^{-3}$ in 4π -steradian.

2.4. Thermal Luminescent Detectors

To estimate the mean energy and intensity of soft x-rays emitted during the glow discharge operation, sensitive Al_2O_3 -based thermoluminescent detectors with a set of $15\text{-}300 \mu\text{m}$ thick ($2.8\text{-}55.5 \text{mg}/\text{cm}^2$) Be-foils were employed. The thermoluminescent detectors register the absorbed radiation dose quantitatively in absolute units while avoiding electrical noise pickup. Seven thermoluminescent detectors, each 5 mm diameter, were located 70 mm from the back side of the anode, outside of the discharge zone. In special experiments to obtain the exact position of the x-ray source in the glow discharge, the molybdenum anode was shifted 20 mm with respect to cathode. In this case, thermoluminescent detectors were exposed directly to the cathode surface. Thermoluminescent detector calibration has been carried out using a standard Cs^{137} gamma source. To read out thermoluminescent detector and analyze the TL-glow-curves, a 2080 TL-Picoprocessor device of Harshaw Co. was used.

2.5. Plastic scintillator detector

Time correlation of x-ray emission with the glow discharge current pulses was studied with a photoelectron multiplier and plastic scintillator (17 mm diameter). These experiments were carried out in a hydrogen atmosphere with a titanium cathode at a pressure of $P = 4.0$ torr and a current of $I = 100$ mA. Detection methods included also a camera obscura designed to image the soft x-rays onto an x-ray film. The camera obscura provides spatial resolution of the x-ray emission, while the scintillation detectors provide temporal resolution of the x-ray emission.

2.6. Proton track detection

Charged particle detection experiments were carried out at voltages ranging from 0.8 to 2.45 kV, and currents ranging from 240 to 450 mA. The duration of each experiment with fixed discharge voltage was $t = 7.0$ h. Preliminary measurements with CR-39 track detectors covered with Al-foils showed statistically significant numbers of 3.0 MeV proton tracks, that depended on the glow discharge voltage and current. Typical distributions of charged particle tracks as a function of the track diameters, dependent on the shielding thickness, for deuterium and hydrogen glow discharges with $U = 1.25$ kV and $I = 240$ mA are shown in Figures 4(a)-4(c). As seen from Fig. 4(a), the track diameter depends strongly on the Al or (Al+PE) shielding thickness in accordance with expected energy losses for 3.0 MeV protons¹⁷ that were generated during deuterium bombardment of titanium cathode. At an Al shielding thickness of $11 \mu\text{m}$, the position of the peak as a function of track diameters occurs at $d = 5.2 \mu\text{m}$ ($E_p = 2.85$ MeV). This peak tends to shift to larger diameters with increasing of shielding thickness, reaching the $d = 6.9 \mu\text{m}$ which corresponds to $E_p = 0.5$ MeV for the shielding $33 \mu\text{m}$ Al + $60 \mu\text{m}$ PE [see Fig.4(c)]. In the case of glow discharge experiments in hydrogen under the same conditions (voltage, current and pressure), no tracks were observed in the range corresponded to 3.0 MeV protons at any shielding thickness [Fig. 4(a)-(c), Ti/H2].

To calculate a thick target yield of 3 MeV protons from the cathode bombarded with deuterons having energy E_d , we used the following formula:³

$$Y_t(E_d) = \int_0^{E_d} N_D(x) \sigma_{\text{lab}}(E) (dE/dx)^{-1} dE, \quad (1)$$

where $N_D(x)$, $\sigma_{\text{lab}}(E)$ and dE/dx are the density of target deuterons in the titanium cathode, the reaction cross section and the stopping power of deuterons in Ti, respectively. The parametrization of Bosch and Hale was used to describe the cross section, with an extrapolation to lower energies that gives good agreement with the gas target experiment.¹⁰ The stopping power of deuterons in the Ti target is assumed to be proportional to the projectile velocity at low deuteron energies.¹⁷

The yields of 3.0 MeV protons obtained at different deuteron energies ranging from 0.8 to 2.45 keV were normalized to those at maximum voltage $U = 2.45$ kV, taking into account the power of discharge or effective temperature at the target surface that both affect the change of effective deuteron concentration in the Ti $N_D(x)$. In this case, the yield should be corrected for the power (effective temperature) applied to the target, reflecting the change in deuterium concentration in the Ti-target: $N_D(\text{eff}) = k(W, T)N_D(x)$, where T and W are the temperature and power at the target surface, respectively that are corresponded to the applied discharge voltage U and current I . The coefficient k can be derived as:¹⁵

$$k(W, T) = \exp \left[-\frac{\varepsilon_d \Delta T}{k_B T_m T_0} \right] \left(\frac{W_m}{W_x} \right), \quad (2)$$

where $\varepsilon_d = 0.04$ eV is the activation energy of deuterons that escape from the Ti

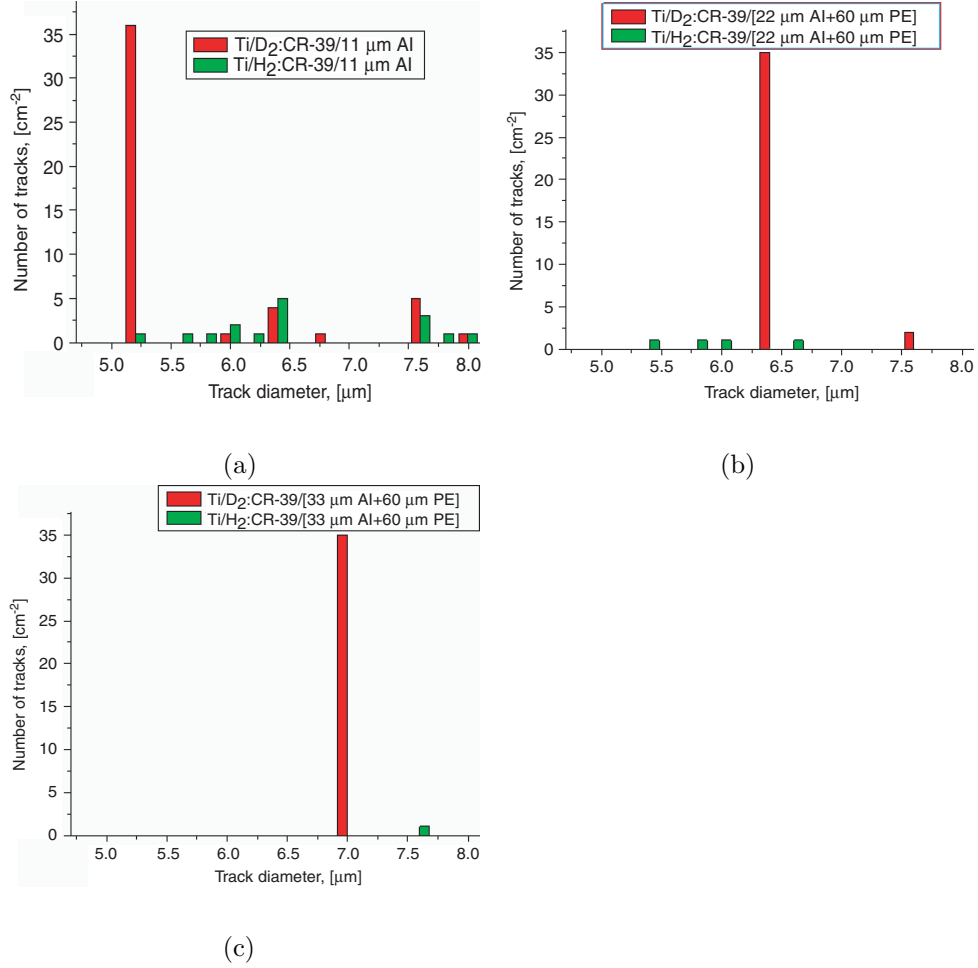


Figure 4. Distributions of track diameters in glow discharge with deuterium and hydrogen at $p = 6.0$ mm Hg; $U = 1.25$ kV; $J = 240$ mA (exposure time $\tau = 7.0$ h); the distance between the detectors and cathode $R = 3.0$ cm: (a) CR-39 detector covered with $11 \mu\text{m}$ thick Al foil. Position of peak at $d = 5.2 \mu\text{m}$ corresponds to 3.0 MeV protons, taking into account the energy loss in $11 \mu\text{m}$ Al is $\Delta E_p = 0.2 \pm 0.1$ MeV); (b): CR-39 detector covered with [$22 \mu\text{m}$ Al foil + $60 \mu\text{m}$ PE film] coating. Position of peak at $d = 6.4 \mu\text{m}$ closely corresponds to 3.0 MeV protons taking (total energy loss in coating is $\Delta E_p = 1.1 \pm 0.2$ MeV); (c): CR-39 detector covered with [$33 \mu\text{m}$ Al foil + $60 \mu\text{m}$ PE film] coating. Position of $d = 6.9 \mu\text{m}$ peak closely corresponds to 3.0 MeV protons (total energy loss in coating is $\Delta E_p = 2.5 \pm 0.2$ MeV).

surface during bombardment; $T_m = 1941$ K is the Ti melting point, $T_0 = 290$ K is the initial target temperature, $\Delta T = T_m - T_0$, $W_m = 906.5$ W is a maximum power at $E_d = eU_m = 2.45$ keV and $I_m = 370$ mA; W_x is the power corresponding to other (lower) voltages and currents in the glow discharge with the titanium target. The value of ε_d was determined from accelerator data⁸, by Arrhenius plotting¹⁸ of 3.0 MeV proton yields for Ti target in the temperature range of 180 - 195 K, at $E_d = 10.0$ keV (with no enhancement) (see Fig. 5).

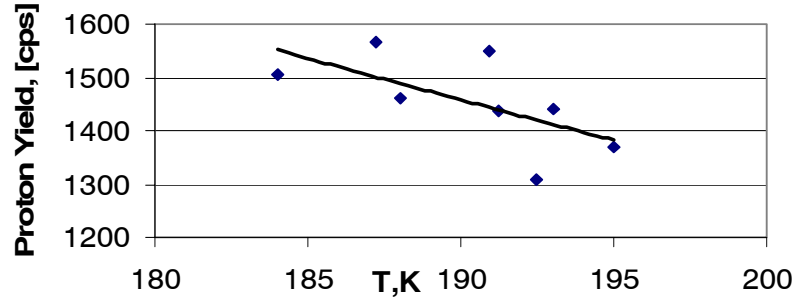


Figure 5. Normalized proton yield in Ti target versus temperature under accelerator deuteron bombardment at $E_d = 10.0\text{keV}$ and $J = 60\text{--}100\mu\text{A}$. Solid line marks an Arrhenius plot.

3. Experimental Results

Measurements with CR-39 track detectors covered with $11\mu\text{m}$ Al-foils showed statistically significant numbers of 3.0 MeV proton tracks, depending on the glow discharge voltage and current. Typical distributions of charged particle tracks as a function of their diameters for a deuterium glow discharge, at two different voltages $U = 2175\text{ V}$ and $U = 805\text{ V}$ at the same current $I = 250\text{ mA}$ are presented in Fig. 6. The position of the 3.0 MeV proton tracks at $d = 5.2\mu\text{m}$ is in good agreement with the calibration data (Fig. 3) and previous measurements at $U = 1.25\text{ kV}$ (Fig. 4). The results, including the number of counts obtained for different deuteron energies and currents, taking into account the temperature correction coefficient k determined according to Eq. (2), are presented in Table 1. As shown in this table, the yield of DD-fusion protons in the energy range of 2.45-0.8 keV decreases about 3 orders of magnitude, taking into account the power and temperature-dependent

Table 1. Specific 3.0 MeV proton yield at different glow discharge voltages $\langle U \rangle$

$\langle U \rangle$ V	$\langle I \rangle$ mA	W_m W	$N(5.2\mu\text{m})$ cm^{-2}	$k(W,T)$	$\langle N_p \rangle$ (cps)	$[\langle n/\varepsilon \rangle \pm \sigma]$ (p/s) in 4π steradian	Y_p (p/C)
805	250	201.3	30	0.0022	2.6×10^{-6}	$(4.7 \pm 1.4) \times 10^{-4}$	0.0019
850	225	191.3	28	0.0016	1.8×10^{-6}	$(3.3 \pm 1.1) \times 10^{-4}$	0.0015
1000	370	370	35	0.036	5.0×10^{-5}	$(9.0 \pm 1.9) \times 10^{-4}$	0.0025
1145	370	420	54	0.053	1.1×10^{-4}	$(2.0 \pm 0.3) \times 10^{-2}$	0.053
1190	240	286	30	0.013	1.6×10^{-5}	$(3.0 \pm 0.5) \times 10^{-3}$	0.013
1435	250	359	50	0.033	7.0×10^{-5}	$(1.3 \pm 0.2) \times 10^{-2}$	0.052
1500	450	675	71	0.16	4.5×10^{-4}	$(8.1 \pm 0.5) \times 10^{-2}$	0.18
1647	300	495	62	0.083	2.1×10^{-4}	$(4.0 \pm 0.5) \times 10^{-2}$	0.13
2000	370	740	159	0.19	1.2×10^{-3}	0.21 ± 0.02	0.57
2175	250	544	252	0.11	1.1×10^{-3}	0.20 ± 0.02	0.80
2450	370	906.5	317	0.27	3.4×10^{-3}	0.61 ± 0.04	1.65

Here $\langle U \rangle$, $\langle I \rangle$ and W_m are the mean discharge voltage, current and amplitude power during discharge operation ($t = 7.0\text{ h}$); N is a 3.0 MeV proton track density in CR-39 detectors; $\langle N_p \rangle$ is a mean count rate of 3.0 MeV protons; $\langle n/\varepsilon \rangle$ is the proton yield in 4π -solid angle, taking into account efficiency $\varepsilon = 5.6 \times 10^{-3}$ of proton detection and Y_p is the specific proton yield per Coulomb of deuteron charge transmitted through titanium cathode.

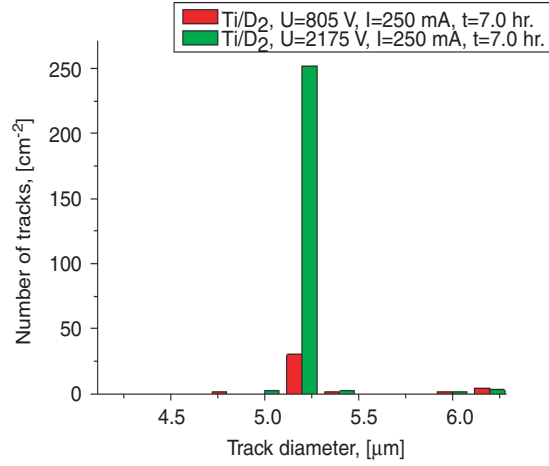


Figure 6. The 3.0 MeV proton yield detected by 11 μm Al covered CR-39 detectors in deuterium glow discharge at the same current and different accelerating voltages: $U_1 = 805 \text{ V}$ and $U_2 = 2175 \text{ V}$.

coefficient k . If the coefficient k were neglected, the yield would be decreased only by one order of magnitude [see column $N(5.2\mu\text{m})$], because the deuterium concentration in the Ti at lower voltage in accordance with Eq. (2) is rather higher than that at $U = 2.45 \text{ kV}$.

3.1. Enhancement factor at low energy

In Fig. 7 the results of normalization of DD-proton yields Y_x at lower energies to those at $E_d = 2.45 \text{ keV}$ are presented and compared to the standard DD-reaction yield behavior (solid line) calculated in accordance with Bosch and Hale DD-cross-section approximation, similarly to Refs. 8 and 9. Even with the total error of measurements, involving as systematic errors of detection and instabilities of the glow discharge ($\pm 10\%$ for current and voltage) as well, the experimental $Y_p/Y(2.45)$ dependence as a function of deuteron energy is well above the standard Bosch and Hale bare approximation curve. This fact definitely indicates presence of a large enhancement of the DD-reaction at the Ti-cathode surface at very low deuteron energy. To estimate the possible enhancement factor $f(E)$ of for the DD-reaction, and the electron screening potential U_s during glow discharge operation for deuterons with energies ranging from 0.8 to 2.45 keV, the following formula³ was applied:

$$f(E) = \frac{Y_p(E)}{Y_b(E)} = \exp \left[\frac{\pi\eta(E)U_e}{E} \right], \quad (3)$$

where $Y_p(E)$ is the experimental yield of DD-protons in glow discharge, $Y_b(E)$ is the bare yield at the same energy determined by Bosch and Hale approximation; $2\pi\eta = 31.29Z^2(\mu/E)^{1/2}$ is the Sommerfeld parameter (here Z is the charge number of deuteron in the case of D^+ projectile and target, μ the reduced mass and E is the

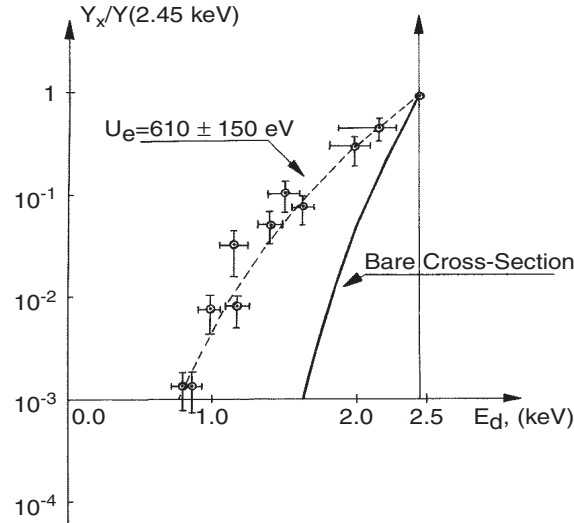


Figure 7. Experimental yield of 3.0 MeV protons at $0.8 < E_d < 2.45$ keV, normalized to that at $E_d = 2.45$ keV. The bare cross-section corresponded to Bosch and Hale approximation to $E_d \leq 2.45$ keV is marked by a solid line. The dashed line is a DD-reaction yield in accordance with a screening potential value $U_e = 610 \text{ eV}$.

center of mass deuteron energy). The data obtained in accelerator⁹ (curve 1) and glow discharge experiments with a titanium target cathode (curve 2) are shown in Fig. 8. In the case of the accelerator measurement with a titanium target at $2.5 < E_d < 10.0$ keV, the deduced screening potential was found to be $U_e = 65 \pm 10 \text{ eV}$.⁹ However, for the glow discharge experiment, the screening potential estimated via enhancement data (curve 2) was found to be as large as $U_s = 620 \pm 140 \text{ eV}$. For instance, this experimental enhancement for glow discharge in terms of DD-proton yield even at $E_d = 1.0$ keV is about nine orders of magnitude larger than that predicted with bare (Bosch and Hale) cross-section (Fig. 8, curve 2).

The glow discharge yields in the range of 0.8-2.45 keV, normalized to that for the accelerator measurement at $E_d = 10.0$ keV (taking into account power and temperature corrections of the glow discharge yield with respect to accelerator), are shown in Figure 9; along with accelerator yields obtained during bombardment of a cooled Ti target.⁸ As in the Fig. 8, the glow discharge yields are much larger than lower energy results deduced from the accelerator data at $U_s = 65 \text{ eV}$.

Thus, the glow discharge low-energy yields, being treated the same way as accelerator data,^{8,9} exhibit larger enhancement at very low D-energy ($E_d < 2.45$ keV) than was expected from the accelerator bombardment. This strong enhancement indicates that at very low-energy range of high-current projectile deuterons, the yields of DD-reaction can be significantly larger than that predicted from the standard (Bosch and Hale) cross-section behavior.

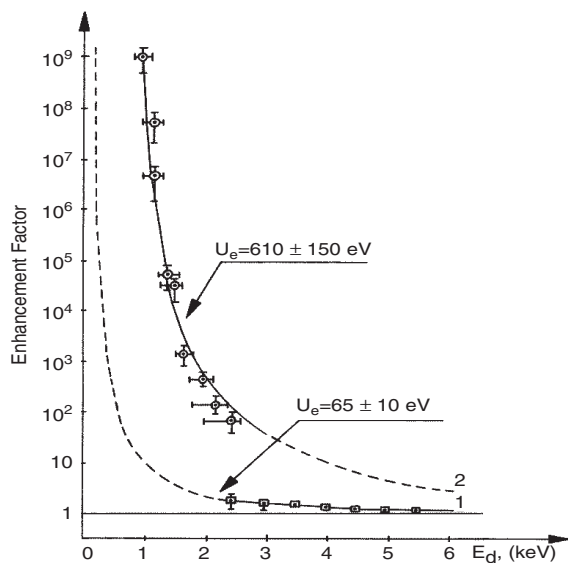


Figure 8. DD-reaction enhancement factor calculated with formula Eq. (3) for the Ti target during deuteron bombardment with accelerator⁹ (curve 1) and glow discharge (curve 2). The solid parts of the curves are corresponded to the deuteron energy ranges where DD-reaction yield was measured experimentally.

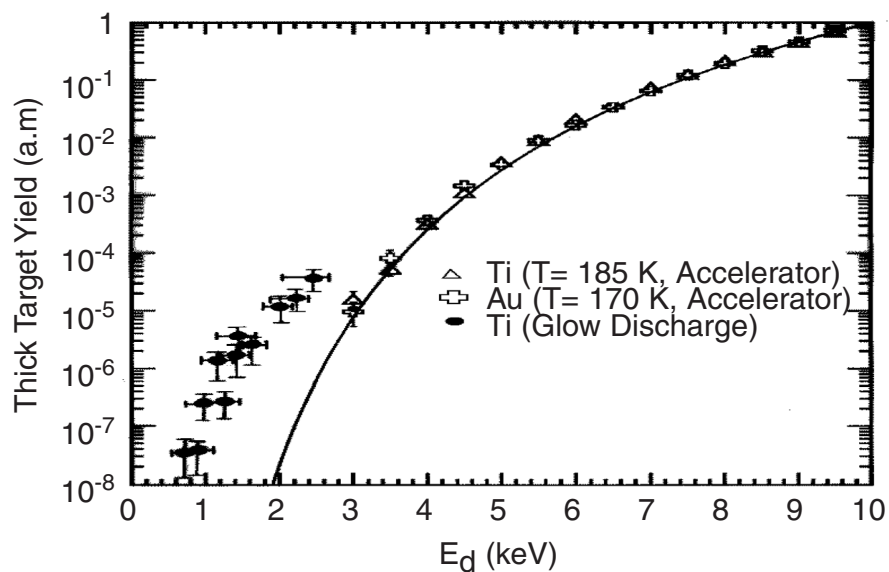


Figure 9. Thick target yields for the glow discharge experiments in D_2 with Ti cathode ($0.8 < E_d < 2.45$ keV) and for accelerator bombardment ($2.5 < E_d < 10.0$ keV) of Ti and Au targets. Both glow discharge and accelerator yields are normalized to that for $E_d = 10$ keV obtained for accelerator bombardment.

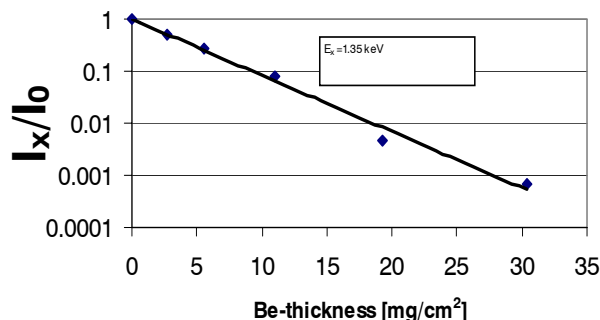


Figure 10. Estimation of x-ray energy (E_x) emitted from the Titanium cathode in a D₂ glow discharge ($U = 1.25$ kV, $J = 200$ mA, $p = 4.4$ mm Hg) using the method of x-ray absorption in Be-foils of different thickness. The thermoluminescent detector spectrometer shown in Fig. 1(b) was employed. I_x and I_0 are the transmitted through the Be-foil and incident x-ray radiation, respectively.

3.2. Soft x-ray emission

Experiments showed that deuteron bombardment of the titanium cathode in the pulsed-periodic glow discharge is always accompanied by intense soft x-ray emission. In the glow discharge experiments involving thermoluminescent detectors with a Ti cathode at $I = 200$ mA and $U = 1.25$ kV, high intensity [$I_x \geq 10^{13}$ photon/s in 4π -steradian] soft x-ray emission with energy $E_x = 1.1 - 1.4$ keV was detected (Fig. 10). It is important that the mean energy of x-ray photons emitted during glow discharge operation is close to the bombarding deuteron energy.

To establish the source of the x-ray in our glow discharge a special movable design of the anode was employed, allowing change the anode position with respect to cathode [Fig. 1(b)]. Using the cathode-anode geometry with “plasma”- anode, (i.e. when the anode is 20 mm shifted aside with respect to cathode) causing the cathode area is fully opened toward the window of the camera obscura with x-ray film, we found that the main fraction of x-ray quanta detected by thermoluminescent detector (>90%) is emitted directly from the Ti-cathode surface. The positive image of x-ray emission from the open cathode taken by the camera obscura (Fig. 11), showed a bright spot comparable with diameter of the cathode area.

The x-ray pulses are strongly correlated with the current pulses in the stationary glow discharge regime. The rise of current and voltage in glow discharge resulted in an essentially nonlinear yield of the x-ray emission (see Fig. 12). The onset of the x-ray signal recorded by the plastic scintillator detector usually coincided with the current pulse start. The x-ray signal reaches its maximum within the time of few μ s, and then drops slowly within 200 μ s duration.

It was found that the energy of x-ray quanta estimated with Be-shielded thermoluminescent detector depended weakly on the discharge voltage (deuteron energy) in the range of 1.2-1.8 kV (Fig. 13). These experiments were carried out at constant discharge current $J = 200$ mA. To change discharge voltage within 1.2-1.8 kV at

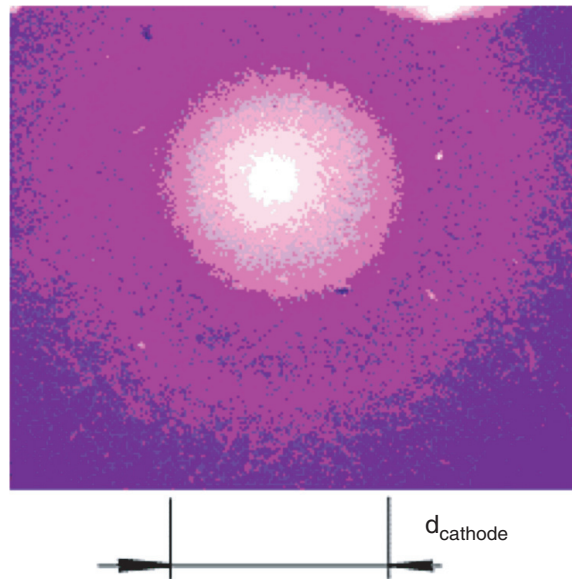


Figure 11. Image of x-ray emission from the titanium cathode using the camera obscura. The 0.3 mm diameter objective is narrowed by the use of a $15 \mu\text{m}$ Be shield in front of the camera. Conditions of the discharge: $J = 150 \text{ mA}$, $U = 1250 \text{ V}$, $p = 5.3 \text{ mm Hg}$; exposure time: 1000 s. The image shown is a positive imprint.

constant current, the deuterium pressure was varied in the range of 2.0-9.0 mm Hg. We found that at $U \leq 1.6 \text{ kV}$, the x-ray quanta energy is about $E_x = 1.22 \pm 0.15 \text{ keV}$, and does not depend significantly on the applied voltage; while at $U > 1.6 \text{ kV}$ the energy tends to increase with voltage reaching $E_x = 1.43 \pm 0.15 \text{ keV}$.

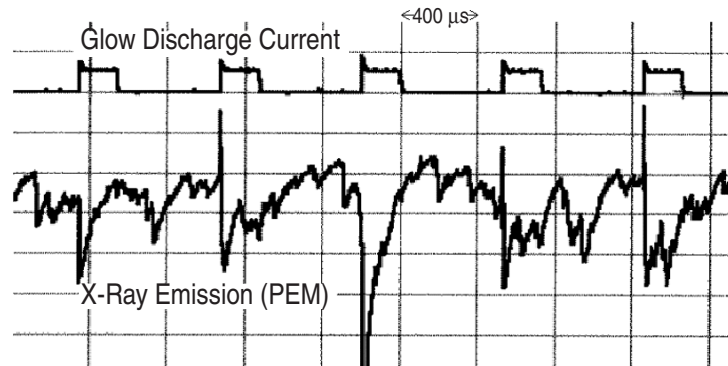


Figure 12. Synchronized time-dependent measurements of the x-ray emission (using the plastic scintillator detector) and the glow discharge pulsed current (pulse duration $\Delta\tau = 400 \mu\text{s}$), in a deuterium glow discharge ($U = 1.4 \text{ kV}$, $J = 250 \text{ mA}$, $p = 4.2 \text{ mm Hg}$).

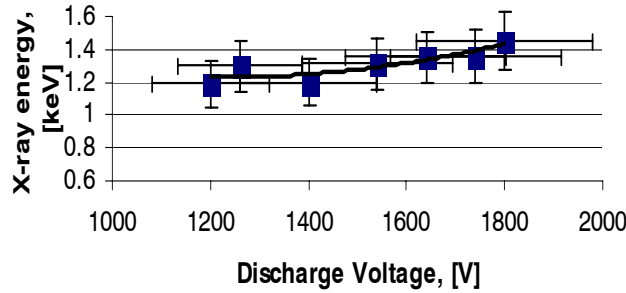


Figure 13. Estimation of a mean x-ray quanta energy, emitted from the Ti-cathode using thermoluminescent detector spectrometer (Fig. 1(b)) in D₂ glow discharge operating at constant current $J = 200$ mA and voltages ranging 1.2–1.8 kV.

3.3. Dependence of soft x-ray emission on discharge power

Measurements of the x-ray dosage absorbed by the thermoluminescent detector, at different currents varying within the range 100–270 mA, and corresponding voltages ranging from 1.0 to 1.8 kV, at constant D₂ pressures $p = 6.0$ and 4.2 mm Hg, showed an exponential increase of yield I_x with increase in effective discharge electric power $P^* = UJQ$ (where $Q = 0.15$ is the constant pulse period-to-pulse duration ratio). This is illustrated in Figure 14. The soft x-ray yield at constant deuterium pressures was found to be in good agreement with a law:

$$I_x = I_0 \exp \left[\frac{\varepsilon}{kT_m} \right] \left(\frac{P^*_x}{P^*_0} \right), \quad (4)$$

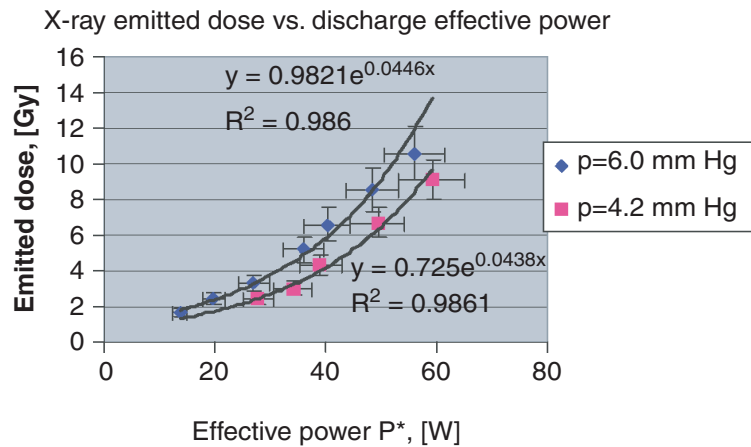


Figure 14. The total doses of soft x-ray quanta emitted by Ti-cathode absorbed by thermoluminescent detector placed at the distance of $r = 7.0$ cm from the cathode for $t = 6000$ s (taking into account the geometry of measurements) versus the discharge effective power $P^* = UJQ$ ($Q = 0.15$ is a pulse on-to-off time ratio) at two different constant pressures: $p_1 = 6.0$ mm Hg and $p_2 = 4.2$ mm Hg.

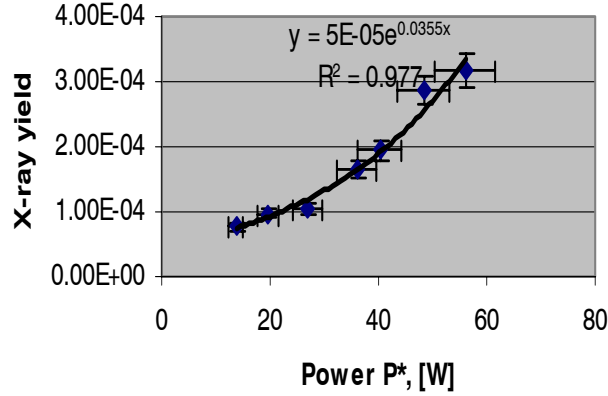


Figure 15. x-ray yield from the Ti cathode at $p = 4.2$ mm Hg per bombarding deuteron versus effective power P^* .

where $I_0 = 0.98$ Gy for $p = 6.0$ mm Hg and $I_0 = 0.725$ Gy for $p = 4.2$ mm Hg, $\varepsilon = 0.04$ eV [the activation energy of deuteron escape from Ti surface (Fig. 5) used for 3.0 MeV proton yield correction to the loss of deuterium concentration via diffusion from Eq. (21)]; $T_m = 1941$ K (Ti melting point) and minimum effective power $P_0^* \cong 6.0$ W for both pressures.

The efficiency of x-ray production per deuteron (representing, in fact, the number of emitted x-ray quanta as a function of discharge current) as a function of the effective power also obeys to the similar exponential law with the same parameters ε , T_m and P_0^* as shown in Figure 15. We note that the x-ray yield in Ti targets will depend strongly on the deuterium concentration at the titanium surface at the melting point, and tends to increase with the effective temperature of the target ($T_{\text{eff}} \sim P^*$).

4. Discussion of Results

So, our study of nuclear and x-ray emission from a titanium cathode in a high-current D-glow discharge, at voltages in the range 0.8-2.45 kV, showed strong DD-reaction enhancement in the Ti cathode accompanied by intense soft x-ray emission. Unlike the accelerator experiments at much lower D^+ beam current and higher deuteron energies,⁶⁻⁹ where a low enhancement ($U_e \leq 60$ eV) was found for titanium, in the present work involving the glow discharge measurement at very low deuteron energies we obtained a remarkably higher screening potential for the titanium cathode.

4.1. Potential sources of error

Let us now consider possible sources of error during low-energy glow discharge experiments that could lead to an overestimation of the screening potential and enhancement in titanium. As was shown in earlier works with accelerators,^{1,3} the

application of the standard procedure of screening potential estimation via thick target yield at different deuteron energies, and comparison of these yields with a Bosch-Hale parametrization, might actually exclude the enhancement errors resulting in the uncertainty of deuterium concentration. The stopping power of deuterons in Ti in our measurements is assumed to be proportional to the projectile velocity v_d , at least down to $E_d = 1.0$ keV, in accordance with existing results for some metals and semiconductors.^{19,20} At the same time, additional measurements of the stopping power at low deuteron energies $E_d \leq 1.0$ keV that can show deviations from the $dE/dx \sim v_d$ law are highly desirable.

The possibility that deuteron channeling might effect the enhancement was considered in Refs. 6 and 7. It was concluded that the channeling phenomenon is not a primary cause of the large observed cross section enhancement due to random orientation of the polycrystalline target as well as radiation damage of the crystalline structure; especially in the case of an intense deuteron flux that leads to large dechanneling of deuterons. We can also exclude the effect of molecular ion component (D_2^+/D_3^+) of the glow discharge as a cause of enhancement overestimation in Ti target because the recent works using both D^+ and D_3^+ projectile ions showed almost the same screening effects.⁶

On the other hand, non-negligible instabilities of both discharge voltage and current, and the high cathode temperature (compared to accelerator experiments) should be considered as a main source of the error in the enhancement estimation during experiments on this glow discharge deuteron bombardment of metal cathode.

Indeed, voltage and current instabilities in our experiments reached about 10% at a stable deuterium pressure. These instabilities lead to increase of experimental errors of the thick target yield and enhancement factor, such that resulting screening potential derived from Eq. (3) was found to be $U_e = 610 \pm 150$ eV, where the deviation $\delta U_e = \pm 150$ eV constitutes about 25% of total U_e and includes corrections from the voltage and current instabilities. Meanwhile, in absence of essential deuteron energy spread in accelerator experiments the uncertainties of screening potential calculation do not exceed of 10%. It should be emphasized that at low deuteron energy $E_d < 5$ keV the screening error in accelerator experiments is mainly determined by the systematic error of detection; due to the relatively low operating beam current, the count rate of DD-reaction products becomes very rare. Contrary, in glow discharge experiment the count rate of DD-reaction 3.0 MeV protons even at $E_d \leq 1.0$ keV is still well above the statistic error due to high deuteron current applied to the target. In any event, our experimental yields of DD-fusion protons from the titanium cathode remains considerably above the standard yield. With decreasing deuteron energy, the difference between experimental and standard yield has tend to increase, significantly exceeding all experimental uncertainties, including errors of detection (Table 1) as well as instabilities of the voltage and current.

In order to use the voltage to control the deuteron energy, the experiments on glow discharge deuteron bombardment were carried out at different deuteron currents (deuterium pressure) and therefore at different discharge power, corresponded

to selected deuteron energies shown in Figs. 7-9. To exclude the effects of discharge power caused by the heating of a subsurface layer (that is comparable in size to the stopping range of the deuterons) which results in a deuteron concentration change during bombardment, we introduced a coefficient $k(W, T)$ [Equation (2)] that takes into account the discharge electric power normalization to the maximal power used at a melting point temperature. Note, that the constant $k(T) = \varepsilon_d \Delta T / k_B T_m T_o$ is about 0.3 and cannot be strongly increased. The reason is that this assumption is based on the fact that the activation energy of deuteron escape from the titanium surface (Fig. 5) has been determined from accelerator data for the low temperature range (170–190 K), and could be considered as a minimal one because activation energy of hydrogen migration at high temperatures has tend only to decrease.²¹ Thus, the correction of the deuteron concentration as a function of the applied discharge electric power that defines the change in deuterium concentration in Ti subsurface layer due to D-diffusion can be considered as a reasonable one. In the absence of this correction, the experimental yields of DD-reaction at lower deuteron energies would be unrealistically increased.

Another possibility exists, which might provide an enhancement of DD-reaction rate due to projectile energy spread by itself, as well as thermal and vibrational motion of target atoms.²² However, using the results of Fiorentini *et al.*²³ it is easy to show that, for instance at $E_d = 1.0$ keV in the case of glow discharge with deuteron energy spread $\Delta E \approx 100$ eV and target atom thermal ($E_{th} \sim 7.0 kT$) and vibrational ($E_{vib} \sim 0.1$ eV²⁰) motion energies, the corresponding total enhancement correction does not exceed about $\Delta f \approx +10\%$. This correction of the enhancement factor $f(E)$, that would increase experimental value could be considered as a marginal one because at $E_d = 1.0$ keV the $f(E)$ number is about 10^9 in accordance with formula Eq. (3). Hence, both a large energy spread and high target temperature compared to accelerator experiments that are observed in the high-current glow discharge experiments cannot explain enhancement deduced from Eq. (3), in terms of a beam width and thermal motion of target atoms.

Therefore, in-spite of additional experimental uncertainties due to peculiarities of glow discharge cathode bombardment compared to accelerator metal target implantation, the data on DD-reaction yields and screening potential obtained in this work plotted in Figs. 7-9 can be considered as reasonable, taking into account possible error analysis.

4.2. Connection between soft x-ray emission and screening

The large enhancement of the DD-reaction with a Ti cathode detected in glow discharge experiments is accompanied by unusually intense x-ray emission from the cathode surface underwent by deuteron bombardment. Such emission was never been observed earlier in low-energy accelerator experiments, perhaps due to small deuteron beam currents and significantly lower specific power applied to subsurface layer of metal target, compared to the glow discharge.

The proof that only x-rays are detected by the thermoluminescent detector

shielded by Be-foils with different thickness can be obtained from the next consideration. In general case, the thermoluminescent detector activation could be carried out either by x-ray, or by electrons with energy in the range of several tens-several hundreds keV. Taking into account the discharge voltage, it is difficult to imagine the possibility of electron acceleration by the energy $E > 10$ keV. On the other hand, electrons possessing an energy $E < 10$ keV should be completely absorbed by the Be foil with thickness $h < 15 \mu\text{m}$. In our case, the radiation detected by thermoluminescent detector decreases essentially (1 order of magnitude) only at an absorber thickness $h > 100 \mu\text{m}$ (Fig. 10). Thus, it can be consolidated that radiation detected by thermoluminescent detector shielded by Be-foils is made up of soft x-rays attenuated by the Be foil in accordance with the x-ray absorption law.

Let us consider possible mechanisms that could involve simultaneous DD-reaction enhancement and soft x-ray emission from the surface of the Ti-target subjected by low-energy deuteron bombardment. Note that so far the screening mechanism of DD-reaction in metals remains a mystery because there is no developed approach to explain $U_e > 100$ eV (strongly above adiabatic limit) by normal valence electron screening.²⁴ Here we note that metal host inner electron shells may somehow to take part in the screening.⁶

In Table 2, the screening potential values for some metal targets, taken mainly from accelerator data obtained by different experimental groups,⁶⁻⁹ including our glow discharge result, are presented and compared to the energies of the closest inner electron shells of corresponding metals. As seen, the screening potential values for these metal targets deduced from the data of different experimental groups are in satisfactorily agreement (within the 1–2 standard deviations) with the energies of electron inner shell of target host atoms.

The proximity of obtained deuteron screening potentials U_s and the energy levels of inner shells of the metal-host targets (in particular, the LII electron shell energy in Ti-atom is consistent with $E_s = 610 \pm 140$ eV) allows us to assume some correlation between the mechanism of deuteron screening and the mechanism of x-ray generation by the Ti-cathode under conditions of dynamical loading with deuterium by

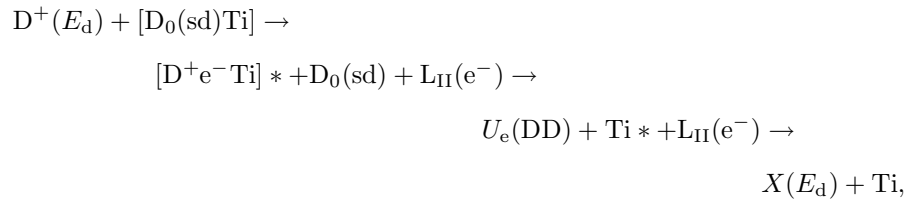
Table 2. Deuteron-deuteron Screening potentials for metal targets.

Target/Ref.	ΔE_d (lab) (keV)	ΔJ (mA)	T (K)	U_e (eV)	Closest metal-host level	E (level) (eV)
Ti ⁷	5–30	0.054	263	≤ 30	Ti (M _{II} /M _{III})	32.6
Ti ⁹	2.5–10.0	0.06–0.25	186	65 ± 15	Ti (M _I)	58.3
Ti*	0.8–2.45	225–450	1941	610 ± 150	Ti (L _{II})	461
Au ⁷	5–30	0.054	263	61 ± 20	Au (O _{II})	71
Au ⁹	2.5–10.0	0.06–0.25	180	70 ± 10	Au (O _{II})	71
Pd ⁷	5–30	0.054	263	800 ± 70	Pd (M _I)	670
Pd ⁹	2.5–10.0	0.06–0.30	313	310 ± 30	Pd (M _V)	334
PdO ⁹	2.5–10.0	0.06–0.30	193	600 ± 20	Pd (M _{II})	560

*Glow discharge measurement.

high-current glow discharge. In this connection, one possible approach to the large deuteron screening in Ti assumes that bombarding deuterons would interact coherently with deuterium flux being massively diffused out of the target (“deuterium fluid”) in the subsurface layer of the Ti-cathode.^{18,25} High diffusivity of deuterium in the glow discharge condition is caused by a high current and temperature in the target layer comparable to the deuteron stopping range. The deuterons diffused in d-metals with high hydrogen affinity should be dynamically bound to the d-valence orbital of metal-host relating in sd-hybridization of valence electrons of deuterium and Ti in the metal outer electron shells.²⁴ We also assume for simplicity that the interaction of the deuteron projectile with the valence shell of Ti bound to another deuteron has an absolutely inelastic character, such that the total projectile energy would be transferred to a wave packet consisting of mixture of D^+ and e- wave functions referenced to a diffusing deuteron bound to sd-hybridized valence orbital of Ti. The projectile deuteron that lost its energy in an inelastic recoil will be stopped, and replace the diffused deuteron near the outer valence orbital of Ti. In that case, the sd-hybridized valence orbital of Ti with attached deuteron would move inside the inner Ti-shell for a short time defined by Heisenberg uncertainty. In fact by this way whole projectile energy at $E_d < 2.0$ keV would be transferred to the inner (LII) Ti shell resulting in a short time LII-electron escape ($\sim 10^{-18}$ s) from its inner level to low-energy state. When this electron returns to its place, it dumps energy gained from the recoiled wave packet in the form of an x-ray quantum.²⁶ Further, the mechanism of such attosecond x-ray emission under the glow discharge deuteron cathode bombardment could be similar to that for the intense laser beam induced attosecond x-ray generation.^{27,28} Under the considered case the energy of emitted x-ray quanta would be equal to projectile energy, assuming absolutely inelastic energy transfer from D^+ -projectile to wave packet formed by Ti atom and deuteron diffused near it.

On the other hand, a strong screening conditions between two deuterons briefly occupying the outer (valence) and the inner-shell orbital would be fulfilled because the barrier reduction between them is exactly the same as the inner LII-shell energy. Moreover, the short time of the process will be enough to allow a DD-reaction. The proposed scheme of processes in the electron shells of Ti-host atom with participation of projectile deuteron D^+ with energy E_d and deuteron diffusing near Ti atom and bound with its d-orbital $D_0(sd)$ can be represented as



where $[D_0(sd)Ti]$ is the hybridized state of electron between diffusing deuteron D_0 and Ti atom; $[D^+e^-Ti]^*$ is the excited state of diffusing deuteron mixed with Ti

d-orbital after projectile strike; $\{L_{II}[D^+ + e^-] + Ti^*D_0(sd)\}$ is the wave packet of mixed D-Ti valence orbital in the inner L_{II} -shell of Ti atom (Ti^* is the excited atom); $U_e(DD)$ is the screening of two deuterons due to one of them is virtually populated the L_{II} - inner shell of Ti-atom; $X(E_d)$ is the x-ray quantum with energy of projectile deuteron E_d .

Under glow discharge deuteron bombardment, the D-diffusion rate in Ti is much faster than in accelerator experiment, due to higher pulsed deuteron current (3-4 orders of magnitude above that for accelerator). The high probability to find a diffusing deuteron near a Ti valence orbital (quasi-liquid flow of deuterium through the Ti lattice) in the glow discharge case would provide much higher probability of quasi-inelastic recoil of a bound deuteron state allowing penetration of deuteron inside the inner L Ti shell. In the accelerator case, the lower concentration and fluidity of deuterons in Ti target causes the elastic projectile to recoil directly on the Ti atom, or a decrease of energy transferred to deuteron bound with Ti valence orbital. Lower residual kinetic energy of the recoiled deuteron does not allow it to reach the L-shell. That is why penetration only into the M-shell would occur, resulting in the low ($U_e \sim 30-60$ eV) screening potential (Table 2).

The proposed model of deuteron screening and x-ray emission under glow discharge bombardment connected to energy transfer from projectile deuteron to deuterons diffused through Ti lattice and sd-bound to valence orbital of Ti atoms, is partially confirmed by the dependence of x-ray yield from the cathode on glow discharge effective power P^* for different deuterium pressures (Fig. 14). The yields of 1.25 ± 0.25 keV x-ray quanta per deuteron for the voltages ranging from 900 to 1700 V also has an exponential dependence on the effective power. Since the temperature over the subsurface layer of Ti-cathode is proportional to the effective power applied to the cathode, the diffusivity of deuterium in this layer should be also proportional to the discharge power. Thus, we conclude that the x-ray emission intensity would increase with the diffusivity of deuterium in the subsurface layer of the cathode.

Regardless of the real mechanism of strong DD-reaction enhancement effect in Ti target accompanying by a high intensity soft x-ray production, the high current pulsed glow discharge could serve as a unique opportunity to study DD-screening at lowest deuteron energies as well as atomic processes in the solids under conditions of high energy density applied.

References

1. U. Greife, F. Gorris, M. Junker *et al.*, *Z. Phys. A* **465**, 150 (1995).
2. M. Junker, A. D'Alessandro, S. Zavatarelli *et al.*, *Phys. Rev. C* **57**, 2700 (1998).
3. H. Yuki, T. Sato, J. Kasagi *et al.*, *J. Phys. G: Nucl. Part. Phys.* **23**, 23 (1997).
4. M. Aliotta, F. Raiola, G. Gyurky *et al.*, *Nucl. Phys. A* **690**, 790 (2001).
5. K. Czerski, A. Hulke, A. Biller *et al.*, *Europhys. Lett.* **54**, 449 (2001).
6. F. Raiola, P. Migliardi, G. Gyurky *et al.*, *Eur. Phys. J. A* **13**, 377 (2002).
7. F. Raiola, P. Migliardi, L. Gang *et al.*, *Phys. Lett. B* **547**, 193 (2002).
8. H. Yuki, J. Kasagi, A.G. Lipson *et al.*, *JETP Lett.* **68**, 785 (1998).

9. J. Kasagi, H. Yuki, T. Baba *et al.*, *J. Phys. Soc. Jpn.* **71**, 2881 (2002).
10. H.S. Bosch and G.M. Hale, *Nucl. Fusion* **32**, 611 (1994).
11. A.B. Karabut, Ya.A. Kucherov, I.B. Savvatimova, *Phys Lett. A* **170**, 265 (1992).
12. V. Violante, A. Torre, G. Silvaggi and G.H. Miley, *Fusion Tech.* **39**, 266 (2001).
13. E.P. Velikhov, A.S. Kovalev and A.T. Rakhimov, *Physical Phenomena in a Gas Discharge Plasma* (Nauka, Moscow, 1987).
14. F.G. Baksht and V.G. Yuriev, *Sov. Tech. Phys.* **49**, 905 (1979).
15. A.G. Lipson, A.B. Karabut and A.S. Roussetski, *Proc. Italian Phys. Soc.* **70**, 335 (2001).
16. K. Oda, M. Ito, H. Miyaki *et al.*, *Nucl. Inst. Meth. B* **35**, 50 (1988).
17. H.H. Anderson and J.F. Ziegler, *Hydrogen Stopping Powers and Ranges in All Elements* (Pergamon, New York, 1977).
18. Y. Fukai and H. Sugimoto, *Adv. Phys.* **34**, 263 (1985).
19. K. Eder, D. Semard, P. Bauer *et al.*, *Phys. Rev. Lett.* **79**, 41129 (1997).
20. S.P. Moller, A. Csete, T. Ichioka *et al.*, *Phys. Rev. Lett.* **88**, 193201 (2002).
21. L. Schlappbach, I. Anderson, J.P. Burger, in *Material Science and Technology, Vol. 3B*. Part II. ed. KH Jurgen Buschow (Weinheim, New York, 1994).
22. C. Bonomo, G. Fiorentini, Z. Fulop *et al.*, *Nuclear Phys. A* **719**, 37C (2003).
23. G. Fiorentini, C. Rolf, F.L. Villante and B. Ricci, *Phys. Rev. C* **67**, 014603 (2003).
24. S. Ichimaru, *Rev. Mod. Phys.* **65**, 255 (1993).
25. D. Pines, *Elementary Excitations in Solids* (J. Wiley, New York, 1963).
26. P.B. Corkum, *Phys. Rev. Lett.* **71**, 1994 (1993).
27. M. Drescher, M. Hentschei, R. Klenberger *et al.*, *Nature* **419**, 803 (2002).
28. A. Batuska, Th. Udem, M. Ulberacker *et al.*, *Nature* **421**, 611 (2003).